Proceedings of 2004 Korea-Japan Joint Seminar
on Particle Image Velocimetry
POSTECH, Korea, Dec. 9 - 10

Visualization of micro-interfacial conditions using Micro PIV

Koji OKAMOTO, Kyosuke SHINOHARA and Yasuhiko SUGII

Dept. Quantum Engineering and Systems Science,
The University of Tokyo,
7-3-1 Hongo, Bunkyo-ku, 113-8656, Japan
okamoto@q.t.u-tokyo.ac.jp

Abstract: A new micro-resolution PIV (Particle Image Velocimetry) has been developed. To investigate transient phenomena in a microfluidic device, Dynamic micro-PIV system was realized by combining a high-speed camera and a CW (Continuous Wave) laser. The technique was applied to a micro-counter-current flow, consisting of water and butyl acetate. The velocity fields of water in the micro counter-current flow were visualized for a time resolution of 500 μs and a spatial resolution of 2.2 x 2.2 μm. Using the Dynamic micro-PIV technique, the vortex-like motions of fluorescent particles at the water-butyl acetate interface were captured clearly.

Keywords: High-speed camera, Transient vortices, Micro counter-current flow, Dynamic Micro PIV

1. Introduction

Microfluidic devices have been applied to many kinds of chemical and biochemical applications including mixing, sorting, enrichment, extraction, heating, and cell cultures. Miniaturization and integration of chemical operations have many specific advantages such as increased speed, efficiency, portability, and reduced consumption through the merits of scale, short diffusion distances and high interface surface-to-volume ratios (e.g., Ho et al., 1998). Microfluidic devices have been utilized for various chemical processing to realize a complicated yet compact chemical system (e.g., Tokeshi et al.,2002). However, several researchers have reported behavior at liquid-liquid interfaces in microfluidic devices, which disagreed with conventional fluid dynamics, for example, the presence of unbalanced shear stresses between miscible liquids (e.g., Sugii et al., 2003) has been reported. It is very difficult to explain all the microfluidic dynamics using conventional theory. Therefore, experimental approaches to the study of microfluidics are very important.

To investigate micro-scale fluidic transport and mixing, the micro PIV (Particle Image Velocimetry) technique has been widely used. The fundamental characteristics of pressure-driven flow (e.g., Meinhart et al., 1999) and electro-osmotic flow (e.g., Devasenathipathy et al., 2002) have been investigated using the micro-PIV technique. In these studies, since the observed region was in the micrometer scale, very short time intervals between two images were necessary for PIV image analysis. To realize short time intervals, double-pulse lasers synchronizing the PIV camera were typically used. Thus, a system consisting of a double pulse laser, a CCD camera, a timing controller, an epi-fluorescent microscope, objective lens, color filters, and optics, was the most popular one used for the micro-PIV systems. In these conventional micro-PIV systems, the time resolution of

velocity distributions was 100 ~ 300 msec, resulting from the frame rate of ordinary CCD cameras such as 4 ~ 10 frame/s.

In the micro-scale, since the Reynolds number is very small, one can assume that the flows were steady in a uniform micro-channel. However, recently, several researchers have reported an apparent transient fluidic phenomenon. Aota et al., (2003) have developed a micro counter-current flow system, which was a water-oil counter flow for highly efficient solvent extraction. The counter-current flow simply cannot and does not exist in the macro-scale because of dominant inertial forces. They observed transient vortex motions of fluorescent particles at the water-oil interface. The understanding of the dynamics is very important for applications of the micro counter-current flow for extraction applications. In order to analyze this transient phenomenon, high time-resolved imaging and longitudinal data are indispensable.

This paper reports a Dynamic micro-PIV technique. A 2000 frame/s high-speed camera under 1024x1024 pixel was equipped with an I.I. (Image Intensifier). Nd:YAG CW single laser were used for illuminating the micro counter-current flow. The proposed Dynamic micro PIV technique was successful in obtaining images of 500 μsec time-series velocity fields, and for capturing the transient vortices at the water-oil interface.

2. High-speed measurement technique

2.1 Experimental setup

Figure 1 shows the experimental setup for the high-speed micro PIV technique. The counter-current flow was visualized using fluorescent particles. The test fluids were pure water and butyl acetate. They were illuminated with a Nd:YAG CW laser (532 nm) from below the microscope stage. The 1 μm particles absorb green light (~535 nm) and emits orange light (~575 nm). The flow images were captured using a high-speed charge-coupled device camera (512 × 512 pixels, 10-bit grayscale, 2000 frames/s) capable of recording 2000 images via an epi-fluorescence microscope equipped with an optical filter (λ = 550 nm) and a water-immersion objective lens (M = 60, NA = 0.9). The depth of field was estimated to be about 5 μm.

2.2 High-speed camera

In order to realize high quality of images and high frame rates simultaneously, the high-speed camera was equipped with a new C-MOS image sensor and a high-capacity memory IC. In this study, the Photron FASTCAM APX with I.I. was used as the high-speed camera. This camera can capture the 1M pixel images with 2000 frame per second. The high-spatial and high-temporal resolutions were simultaneously achieved. Using the camera, much higher frame rate may also be achieved, e.g., 512x512 pixel with 6000fps. Since the exposure time of 500 μs (2000fps) was very short due to the high frame rate, the intensity of the images was too dark to record. We applied an image intensifier to the high-speed camera. The image intensifier used an optic fiber coupling. Its resolution and decay time were 32 lp/mm and 6 μs, respectively. As a result, the high-speed camera could capture very weak luminance.

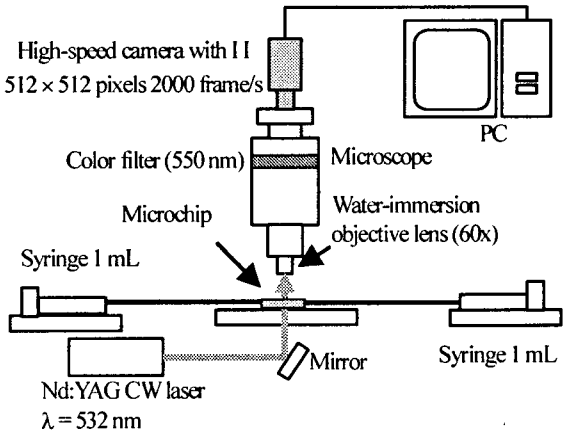

Fig.1 Experimental setup for the Dynamic micro-PIV system

2.3 Microchannel

The test section was a counter-cross channel. Figure 2 shows a schematic of the microfluidic device. The micro channels were 100 μm in width and 25 μm in depth (semi-circular profile). The microchannels were fabricated on a pylex glass microchip by a photolithography wet etching technique (e.g., Aota et al., 2003). The top side of the channel was closed by a cover glass. Two channels were connected to one channel in an x configuration, and the two input and the two output channels could be fed independently. The length and depth of the contiguous section between the upper channel and the lower channel were 500 and 15 μm, respectively. In order to realize a stable counter-current flow, hydrophilic/hydrophobic characteristics for the microchannel walls were utilized. The wall of upper channel for the organic solution was hydrophobic by modifying it with octadecylsilane groups (e.g., Hibara et al., 2002). Conversely, the wall of lower channel for the aqueous solution was hydrophilic because of the normal surface character of bare glass.

Water flowed from the lower right input to the lower left output, and butyl acetate flowed from the upper left input to the upper right output, as shown in figure 2. The density, viscosity, surface tension, and refractive index of pure water at 20 °C are 1.00×10^3 kg/m^3, 0.89×10^{-3} Pa s, 72.0×10^{-3} N/m, and 1.33, respectively. In case of butyl acetate, they are 0.88×10^3 kg/m^3, 0.69×10^{-3} Pa s, 24.9×10^{-3} N/m, and 1.39 respectively. The solubility of butyl acetate in water is 2.3 wt %, indicating that they are almost immiscible. The test fluids were introduced into the channels using 1 mL capacity syringes and syringe pumps. The flow rates of water and butyl acetate were fixed to be (a) 1.0 μL/min and 1.5 μL/min and (b) 0.1 μL/min and 1.3 μL/min, respectively. The corresponding Reynolds numbers are $\rho UL/\mu$ = w: 0.75 -b: 1.3 and w: 0.075-b: 1.1, respectively where ρ is the density, μ is the viscosity, U is the axial average velocity, and L is the width between the channel wall and the interface. The fluorescent particles were seeded into water at a concentration of 0.4% by volume, and they dispersed uniformly. Conversely, since the particles do not disperse in butyl acetate, they were not available for butyl acetate.

Figure 3 shows the observation region illuminated by a halogen lamp. This was an area of 190 × 190 μm immediately downstream to the junction such that the length between the left edge of the image and the left confluence point of the channels was 10 um. Each pixel in the captured image represents an area of 0.37 × 0.37 μm. The focal plane was set at 7 μm depth from the top wall. In the upper channel, butyl acetate flowed from the left side to the right side, and in the lower channel, water flowed from the right side to the left side. In the center of the channel, a stationary interface between water and butyl acetate was observed. It was observed as a black layer due to the difference in refractive index. In order to stabilize the interface, the chemical surface modification was applied to the upper channel, and the guide structure was set at the center of the microchannel described as the cross section in Figure 2. Since surface tension is dominant in the microscopic scale, the interface between organic solution and water was fixed at the edge of the guide and the center of the top wall. Therefore, although the flow rate of butyl acetate was very different from

that of water, the stable interface was observed at the center of the channel. The inner wall of the channel was clearly observed in the horizontal profile. However, as the channel wall was inclined gently, each wall was also observed as a black layer due to refraction. Since the frame rate of 2000 Hz was very high, each flowing fluorescent particle was clearly visualized as a black point in the water by the transmitted light. Figure 4 shows an image of the fluorescent particles. The particles, which were distributed randomly in water, appeared as bright points. The two white lines represented the outline of inner walls. The outline of the lower wall and the interface were recognized by the boundary between the bright region and the dark region. Since the refractive index of glass (1.46) is close to that of water (1.33), the particles near the wall or the interface were observed clearly. The particle diameter in the images was 7 or 8 pixels.

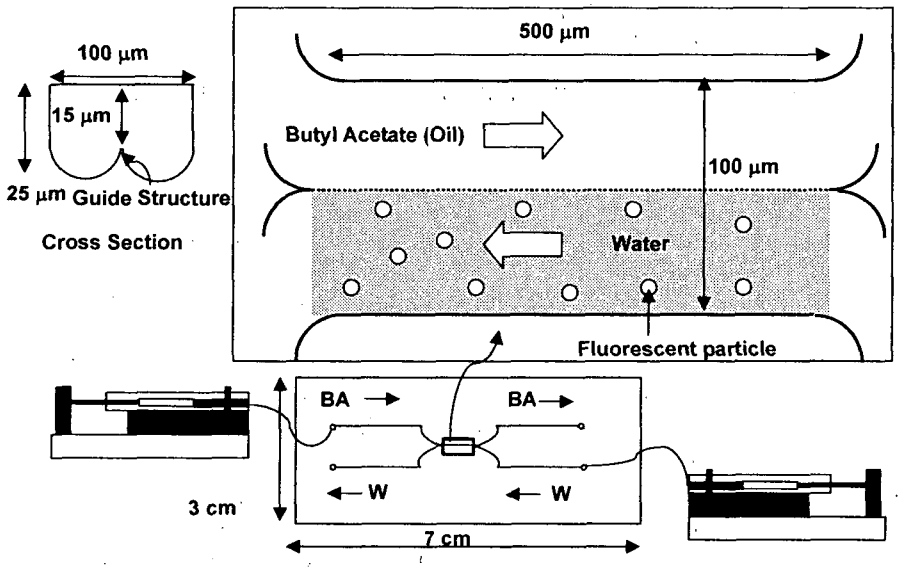

Fig.2 Schematic of a microfluidic device.

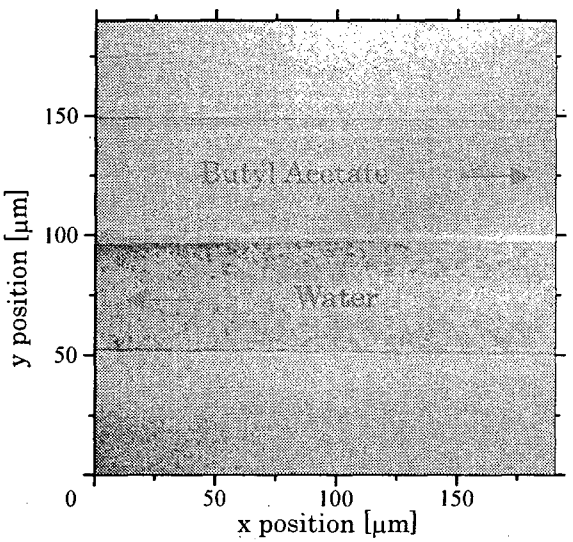

Fig.3 Measurement region

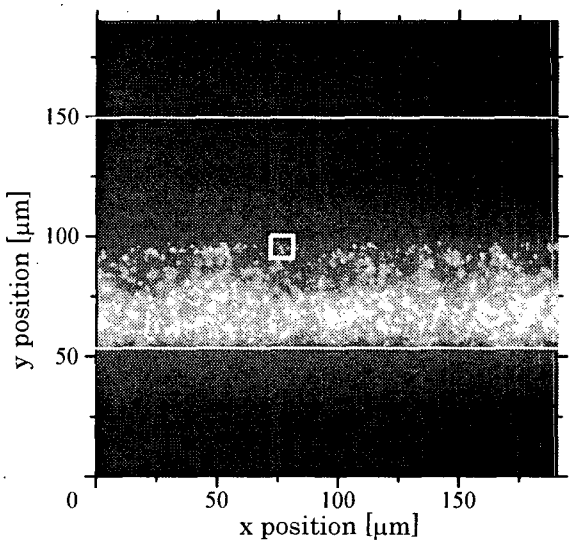

Fig.4 Fluorescent particle image

3. Results and discussion

3.1 Time-averaged velocity distributions

In order to investigate the fundamental characteristics of the velocity field, the time-averaged velocity field was analyzed. Figure 5 shows the time-averaged velocity distributions in (a) w: 1.0 μL/min-1.5 μL/min and (b) w: 0.1 μL/min-1.3 μL/min. The velocity distributions were obtained by averaging 2000 images for 1.0 sec using the PIV technique (e.g., Sugii et al., 2000). The integration window was taken as 12 × 12 pixels with 50% overlap, corresponding to a spatial resolution of 2.2 × 2.2 μm. The max velocity vectors were observed at the middle of the water flow, and the velocity near the wall was close to zero. In case (a), the velocities at the interface were almost zero and the boundary looked straight. Conversely, in case (b), a downward-curved velocity field was observed from x = 75 to 125 μm. This indicated that the clockwise motions of particles were generated more repeatedly in this area.

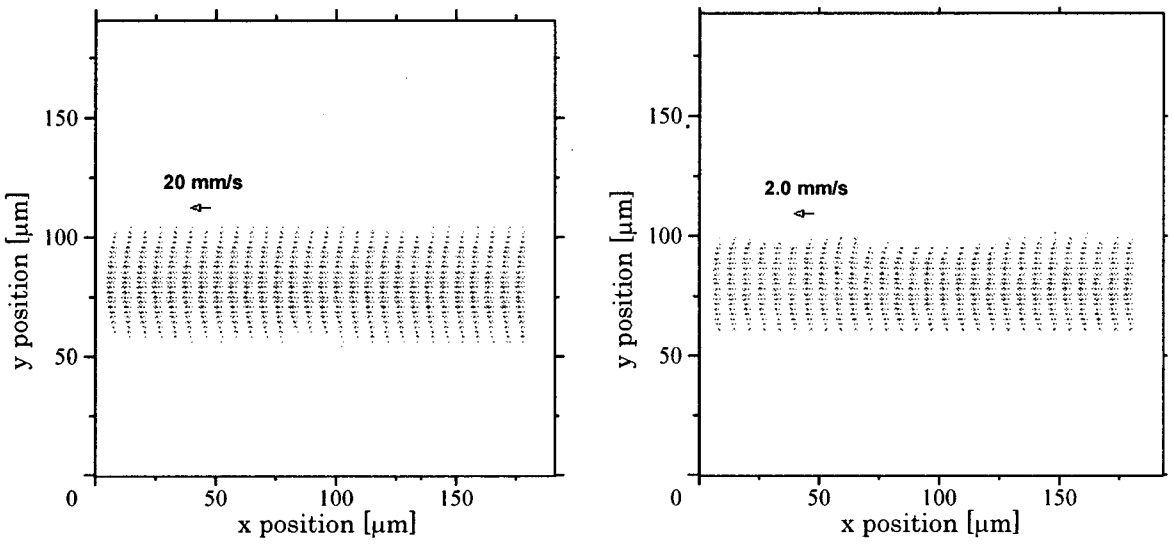

(a) Time-averaged velocity distribution under Re_w = 0.75

(b) Time-averaged velocity distribution under Re_w = 0.075

Fig.5 Time-averaged velocity distributions of 1000 images for 0.5 sec. The horizontal axis is x position [μm], and the vertical axis is y position [μm]. Re_w is Reynolds number of water flow.

3.2. Velocity profiles

Figure 6 shows time-averaged velocity profiles. The horizontal axis is y position [μm], and the vertical axis is the axial velocity [mm/s]. The gray, black, and white dots represented upstream, middle, and downstream, respectively. Each position was for x = 50, 100, and 150 μm. The error bars represent the time variance of the 1000 images. In case (a), the maximum velocity was about 18 mm/s at y = 80 μm. At the wall and at the interface, the velocity was close to zero. The temporal variations were about 1 % of the time-averaged velocity. Conversely, in case (b), the maximum velocity was about 1.8 mm/s at y = 80 μm. At the wall, the velocity was almost zero. The temporal variations were about 5 % of the time-averaged velocity. At the interface, the variations were bigger. Since there were no fluorescent particles on the oil side, the interface in the PIV image was treated as a wall (Figure 4). However, the near-interface variances were bigger than those near the wall. This indicates that the fluctuations in the near-interface flow were larger due to the vortex-like motions.

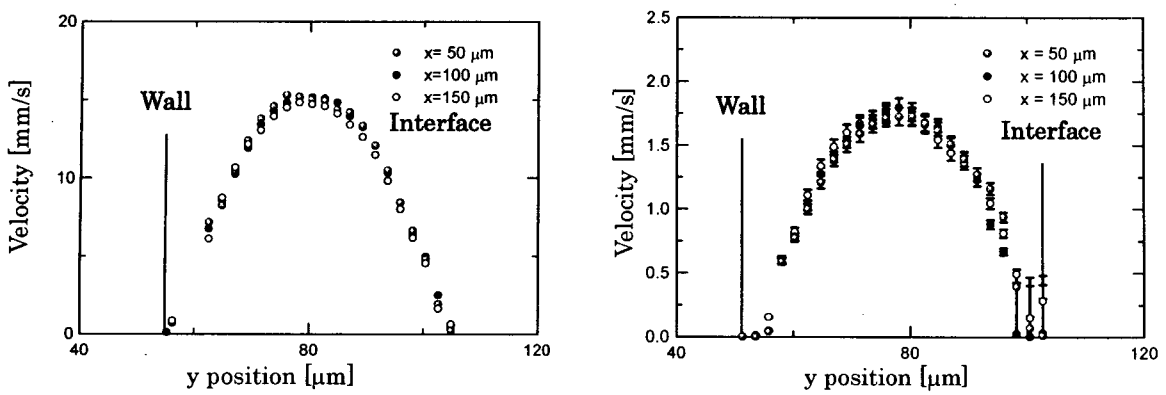

(a) Time-averaged velocity distribution under Re_w = 0.75

(b) Time-averaged velocity distribution under Re_w = 0.075

Fig.6 Time-averaged velocity profiles of 1000 images for 0.5 sec. The horizontal axis is y position [mm], and the vertical axis is the axial velocity [mm/s]. The gray, black, and white dots represented upstream, middle, and downstream, respectively.

3.3 Time evolution of the flow

Figure 7 shows close-ups of the near-interface flow in case (b) w: 0.1 μL/min-1.3 μL/min. The observed region was the heavy-line frame shown in Figure 4. The images on the left are time-series fluorescent particle images for 1.5 ms, and the images on the right are instantaneous velocity fields analyzed by two fluorescent images. Their size is 12 × 12 μm and t was the time. In the upper area, the two fluorescent particles marked by the triangles flowed from the left side to the right side. Conversely, the two fluorescent particles marked by the squares flowed from the right side to the left side. The right-pointing vectors and left-pointing vectors were observed in the upper area and the lower area, respectively. With time, the flow field turned gradually from a crossed one to a rotating one. This motion showed the vortex-like motion. Furthermore, the particles moving left were observed to be smaller than those moving right. This indicated that each particle might flow at different depths, and the near-interface flow field might be three-dimensional.

4. Conclusion

A high-speed micro PIV technique has been developed to measure transient fluidic phenomena in a microfluidic device, and the dynamics of counter-current flow were investigated. The system, consisting of an epi-fluorescent microscope, CW laser, and a high-speed CMOS camera, was applied to the analysis of velocity fields of water containing fluorescent particles in a counter micro-channel. The fluorescent particle images were analyzed by the highly accurate PIV method, and time-series velocity distributions were obtained with a 500 μs time resolution and 2.2 × 2.2 μm spatial resolution. The velocity profiles of water between the interface and the wall were obtained, and vortex-like motions around the interface were captured clearly. The high-speed micro PIV technique will be strong method for measurement of transient fluidic phenomenon in microscopic scale.

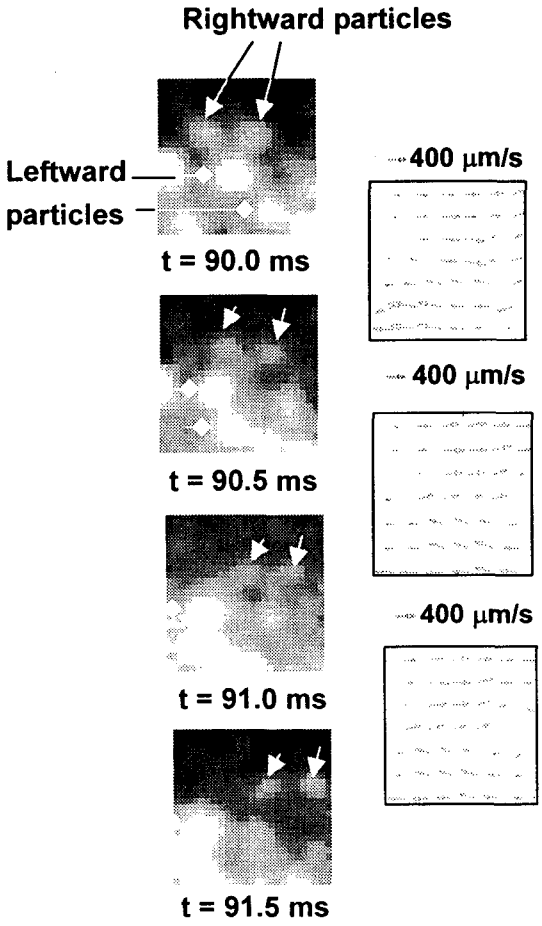

Fig.7 Time evolution of close-up of the near-interface flow in the heavy-line frame shown in Figure 4. The size of the close-ups was 12 × 12 μm and t was the time. The left images were fluorescent particle images, and the right images were instantaneous velocity distributions. The integration window was taken as 12 × 12 pixels with 50% overlap, corresponding to a spatial resolution of 2.2 × 2.2 μm.

References

Aota, A., Nonaka, M., Hibara, A., Kitamori, T., 2003, "Micro counter-current flow system for highly efficient extraction", Proc. Micro-TAS 2003 Squaw Valley USA, 441.

Devasenathipathy S., Santiago J.G., Takehara, K., 2002, "Particle tracking techniques for electrokinetic microchannel flows", Anal. Chem., Vol.74, 3704.

Hibara, A., Nonaka, M., Hisamoto, H., Uchiyama, K., Kikutani, Y., Tokeshi, M., Kitamori, T., 2002, "Stabilization of Liquid Interface and Control of Two-Phase Confluence and Separation in Glass Microchips by Utilizing Octadecylsilane Modification of Microchannels", Anal. Chem., Vol.74, 1724.

Ho C. M., Tai Y. C., 1998, "Micro-electro-mechanical systems (MEMS) and fluid flows", Ann. Rev. Fluid Mech. Vol. 30, 579.

Meinhart C.D., Wereley S.T., Santiago J.G., 1999, "PIV measurements of a microchannel flow", Exp. Fluids, Vol.27, 414.

Meinhart C. D., Wereley S. T., Gray M. H. B., 2000, "Volume illumination for two-dimensional particle image velocimetry", Meas. Sci. Technol., Vol.11, 809.Sugii, Y., Okamoto, K., Hibara, A., Tokeshi, M., Kitamori, T., 2003, "Stabilization of interface between two liquid phases on a microchip by means of micro PIV technique", Proc. PSFVIP-4, Charmonix, France

Santiago J. G., Wereley S. T., Meinhart C. D., Beebe D. J., Adrian R. J., 1998, ``A particle image velocimetry system for microfluidics'', Exp. Fluids, Vol.25, 316.
Sugii, Y., Nishio, S., Okuno, T., Okamoto, K., 2000, ``A highly accurate iterative PIV technique using gradient method'', Meas. Sci. Technol., Vol.11, 1666.
Tokeshi, M., Minagawa, T., Uchiyama, K., Hibara, A., Sato, K., Hisamato, H., Kitamori, T., 2002, ``Continuous-flow chemical processing on a microchip by combining microunit operations and a multiphase flow network'', Anal. Chem., Vol.74, 1565.